Proc. Natl. Acad. Sci. USA
Vol. 95, pp. 15043–15048, December 1998
Neurobiology

The neuropeptide Y/agouti gene-related protein (AGRP) brain circuitry in normal, anorectic, and monosodium glutamate-treated mice

(arcuate nucleus/coexistence/feeding/melanocortin/parabrachial nucleus)

CHRISTIAN BROBERGER*†, JEANETTE JOHANSEN‡, CAROLINA JOHANSSON‡, MARTIN SCHALLING‡, AND TOMAS HÖKFELT*

Departments of *Neuroscience and ‡Molecular Medicine, Karolinska Institutet, 171 77 Stockholm, Sweden

Contributed by Tomas Hökfelt, October 19, 1998

ABSTRACT **Neuropeptide Y (NPY) and the endogenous melanocortin receptor antagonist, agouti gene-related protein (AGRP), coexist in the arcuate nucleus, and both exert orexigenic effects. The present study aimed primarily at determining the brain distribution of AGRP. AGRP mRNA-expressing cells were limited to the arcuate nucleus, representing a major subpopulation (95%) of the NPY neurons, which also was confirmed with immunohistochemistry. AGRP-immunoreactive (-ir) terminals all contained NPY and were observed in many brain regions extending from the rostral telencephalon to the pons, including the parabrachial nucleus. NPY-positive, AGRP-negative terminals were observed in many areas. AGRP-ir terminals were reduced dramatically in all brain regions of mice treated neonatally with monosodium glutamate as well as of mice homozygous for the anorexia mutation. Terminals immunoreactive for the melanocortin peptide α-melanocyte-stimulating hormone formed a population separate from, but parallel to, the AGRP-ir terminals. Our results show that arcuate NPY neurons, identified by the presence of AGRP, project more extensively in the brain than previously known and indicate that the feeding regulatory actions of NPY may extend beyond the hypothalamus.**

Neuropeptide Y (NPY) (1)-producing neurons in the hypothalamic arcuate nucleus (2, 3) appear to be involved in the regulation of feeding behavior. Intracerebral injections of NPY induce food intake (4, 5), and starved animals increase NPY expression (6, 7). In genetic models of feeding disorders, arcuate NPY overexpression has been linked to hyperphagia and obesity (8), and NPY deficiency has been linked to hypophagia and anorexia (9). However, surprisingly little information is available on the arcuate NPY projections, and targets for these neurons so far have been demonstrated only in a limited number of hypothalamic nuclei (10–12). Recently, Hahn *et al.* (13) and we (14) have reported that many NPY neurons in the rodent arcuate coexpress agouti gene-related protein (AGRP) (15), an endogenous antagonist of the anorexigenic melanocortin peptides, e.g., α-melanocyte-stimulating hormone (αMSH) (16, 17). The present study aimed at investigating whether AGRP expression is limited to arcuate NPY neurons, using double-labeling immunohistochemistry and *in situ* hybridization. If so, AGRP staining could be used to map the terminal projections of arcuate NPY neurons. To further ascertain the arcuate origin of AGRP-immunoreactive (ir) terminals, we also analyzed mice treated neonatally with monosodium glutamate (MSG), which induces necrosis of arcuate neurons (18), including the NPY cells (11, 19). In addition, we studied AGRP in the mutant anorexia (*anx/anx*) mouse, where abnormalities in arcuate NPY histochemistry have been demonstrated (9).

MATERIALS AND METHODS

Animals. C57Bl6 mice (B&K Universal, Sollentuna, Sweden) were injected s.c. with MSG (Sigma) at doses of 2.2, 2.5, 2.8, 3.2, 3.4, 3.6, 3.8, 4.0, and 4.2 mg/g or 0.9% NaCl (vehicle) on postnatal days 2–10, respectively (20). Four MSG-treated mice and their controls were perfused at 70–80 days of age. *anx/anx* mice and control littermates were genotyped by nearby simple-sequence-length polymorphisms and perfused at day 20. For immunohistochemical labeling of arcuate cell bodies, three normal, two vehicle-treated, and two MSG-treated male mice were injected intracerebroventricularly with 60 μg colchicine in 10 μl 0.9% NaCl 24 h before perfusion. Mice were anesthetized with sodium pentobarbital (Mebumal i.p.) and perfused via the ascending aorta with formalin-picric acid. The brains were dissected out, immersion-fixed, and rinsed (9). For *in situ* hybridization, brains were dissected from decapitated animals and frozen.

***In Situ* Hybridization.** Brains were mounted on chucks, frozen, and sectioned at 14 μm. Oligonucleotide probes complementary to nucleotides 1–48 of mouse AGRP mRNA (B. D. Wilson, J. Kerns, M. M. Ollmann, and G. S. Barsh, GenBank accession no. 489486, 1997) and nucleotides 1297–1344, 1581–1624, and 1671–1714 of the rat preproNPY mRNA (21) were synthesized (Scandinavian Gene Synthesis, Köping, Sweden). The AGRP probe was 3′ end-labeled with [α-^{35}S]dATP (NEN) by using terminal deoxynucleotidyl transferase (Amersham) to a specific activity of 4.2×10^6 cpm · ng^{-1} oligonucleotide and purified by using Qiaquick Nucleotide Removal Kit (Qiagen), and the NPY probes were labeled by tailing the 3′ end with digoxigenin-11-dUTP according to published protocols (22), purified by ethanol precipitation, and dissolved in Tris-EDTA, all as described earlier (23). *In situ* hybridization was performed essentially as described previously (23–25). The sections were incubated with radioactively labeled AGRP probe and digoxigenin-labeled NPY probes. After hybridization, the sections were rinsed and incubated overnight with alkaline-phosphatase-conjugated antidigoxigenin F(ab) fragment (1:5,000; Boehringer Mannheim). Alkaline phosphatase activity was developed by incubating the sections with nitroblue tetrazolium/5-bromo-4-chloro-3-indoyl phosphate *p*-toluidine salt (GIBCO/BRL). The sections were

The publication costs of this article were defrayed in part by page charge payment. This article must therefore be hereby marked "*advertisement*" in accordance with 18 U.S.C. §1734 solely to indicate this fact.

Abbreviations: AGRP, agouti gene-related protein; αMSH, α-melanocyte-stimulating hormone; MSG, monosodium glutamate; NPY, neuropeptide Y; NTS, nucleus tractus solitarii; PBN, parabrachial nucleus; PVH, paraventricular hypothalamic nucleus; -ir, -immunoreactive; -LI, -like immunoreactivity.

†To whom reprint requests should be addressed.

air-dried, dipped in Ilford K5 nuclear emulsion, exposed for 1 week, developed and fixed, or exposed to autoradiographic film (Amersham), which was developed after 4 days. Autoradiograms were quantified with NIH IMAGE software (W. Rasband, National Institute of Mental Health) as described (9). For further details see ref. 23.

Immunohistochemistry. Fourteen-micrometer-thick brain sections were incubated with monoclonal mouse NPY antibodies (1:400) (26) and/or polyclonal rabbit antiserum to AGRP (1:4,000, Phoenix Pharmaceuticals, St. Joseph, MO) or αMSH (1:4,000; Peninsula Laboratories), rinsed, incubated with fluorescein isothiocyanate-conjugated secondary antibodies (1:80, Jackson ImmunoResearch) for NPY staining, and processed by using the catalyzed reporter-deposition method and Renaissance kit (NEN) for AGRP or αMSH staining as described previously (14). Sections were incubated with a 1:50 dilution of biotinyl tyramide (NEN), and deposited biotin was detected with Texas red-conjugated streptavidin (1:200; Amersham). Finally, the sections were rinsed, mounted, and examined in a Nikon Microphot FX microscope equipped for epifluorescence with an oil dark-field condenser and proper filters. Kodak T-MAX 100 film was used. The stereotaxic atlas of Franklin and Paxinos (27) was consulted. For quantification of nerve terminal arborizations, a grid with 1.0-mm side length of individual squares (Graticules, Tonbridge, U.K.) was placed in the eye-piece. The dorsal part of the dorsomedial hypothalamic nucleus was selected for quantification, and the number of crossings between fibers and grid lines was counted in sections from both *anx/anx* and wild-type littermates through a ×40 objective. Statistical analysis was carried out by using ANOVA and Mann–Whitney *U* test. Values are presented as ±SEM.

Controls. For *in situ* hybridization, sections were incubated with an excess (100×) of unlabeled probe. The specificity of the AGRP antiserum has been reported elsewhere (14).

RESULTS

***In Situ* Hybridization.** After double-labeling *in situ* hybridization, an almost complete coexpression of NPY and AGRP mRNA in arcuate neurons of C57Bl6 mice could be observed; 94.9 ± 1.5% of NPY mRNA-positive cells expressed AGRP mRNA, and 98.4 ± 0.3% of AGRP mRNA-positive cells expressed NPY mRNA ($n = 4$; Fig. 1 *a–e*). AGRP mRNA was not detected in any other region of the brain examined, including the olfactory bulb, striatum, cerebral and cerebellar cortices, preoptic area, thalamus, hypothalamus, mesencephalon, pons, brainstem, and spinal cord. Hybridization in the presence of unlabeled probe abolished the signals.

Immunohistochemistry. AGRP-ir cell bodies could be detected only in the arcuate nucleus of colchicine-treated mice. The vast majority of NPY-ir cell bodies also contained AGRP-like immunoreactivity (-LI) and all AGRP-ir cell bodies contained NPY-LI (Fig. 1 *f* and *g*). AGRP-ir terminals were detected in several brain areas, and they always contained NPY-LI (cf. Fig. 2 *a*, *c*, *e*, and *m* with *b*, *d*, *f*, and *n*, respectively). Many NPY-ir terminals did not contain AGRP-LI. In some instances, e.g., on the interface between the bed nucleus of the stria terminalis and the nucleus accumbens, an AGRP-ir/NPY-ir population of terminals was seen bordering to an AGRP-negative/NPY-positive population of terminals (cf. Fig. 2 *c* with *d*).

In the telencephalon, low-density terminal networks were observed in the medial and posterior anterior olfactory nucleus, medial orbital cortex, and tenia tecta. No terminals were observed in the olfactory bulb. No AGRP-LI was observed in the NPY-ir terminals in the cerebral cortex, hippocampus, nucleus accumbens, or the caudate putamen. A moderately dense fiber network was located in the lateral septal nucleus, especially medially. The bed nucleus of the stria terminalis contained a high-density network of terminals; however, the NPY-ir perikarya located in this nucleus did not stain for AGRP (cf. Fig. 2 *c* with *d*). AGRP-ir fibers traveled through the stria terminalis to provide moderately dense networks in the posterodorsal medial and central nuclei of the amygdala. Fibers also were seen running along the external capsule.

In the diencephalon, the hypothalamus was densely laden with AGRP-ir terminals, paralleling that of NPY-LI, but only

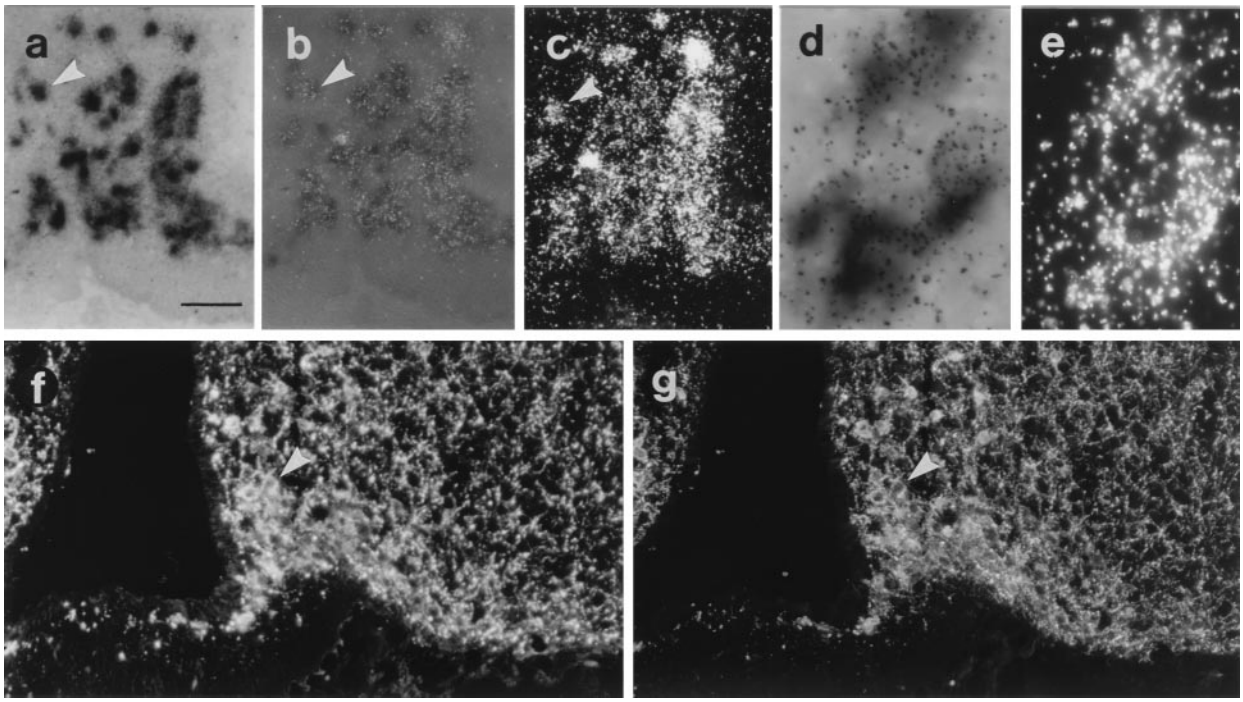

FIG. 1. Micrographs from mouse arcuate nucleus sections processed for *in situ* hybridization (*a– e*) or immunohistochemistry (*f* and *g*) double-labeling for AGRP or NPY mRNA (*a– e*) or peptide (*f* and *g*), respectively. Micrographs taken with bright-field (*a* and *d*), bright-field with epiillumination (*b*), dark-field (*c* and *e*), or fluorescence illumination (*f* and *g*). NPY mRNA visualized as dark precipitate (*a*, *b*, and *d*) and AGRP mRNA detected as silver grains (*b*, *c*, and *e*) are shown. Note coexistence of AGRP and NPY mRNA/peptide in cell bodies (arrowheads). [Bar = 50 μm (*a–c*, *f*, and *g*) and 250 μm (*d* and *e*).]

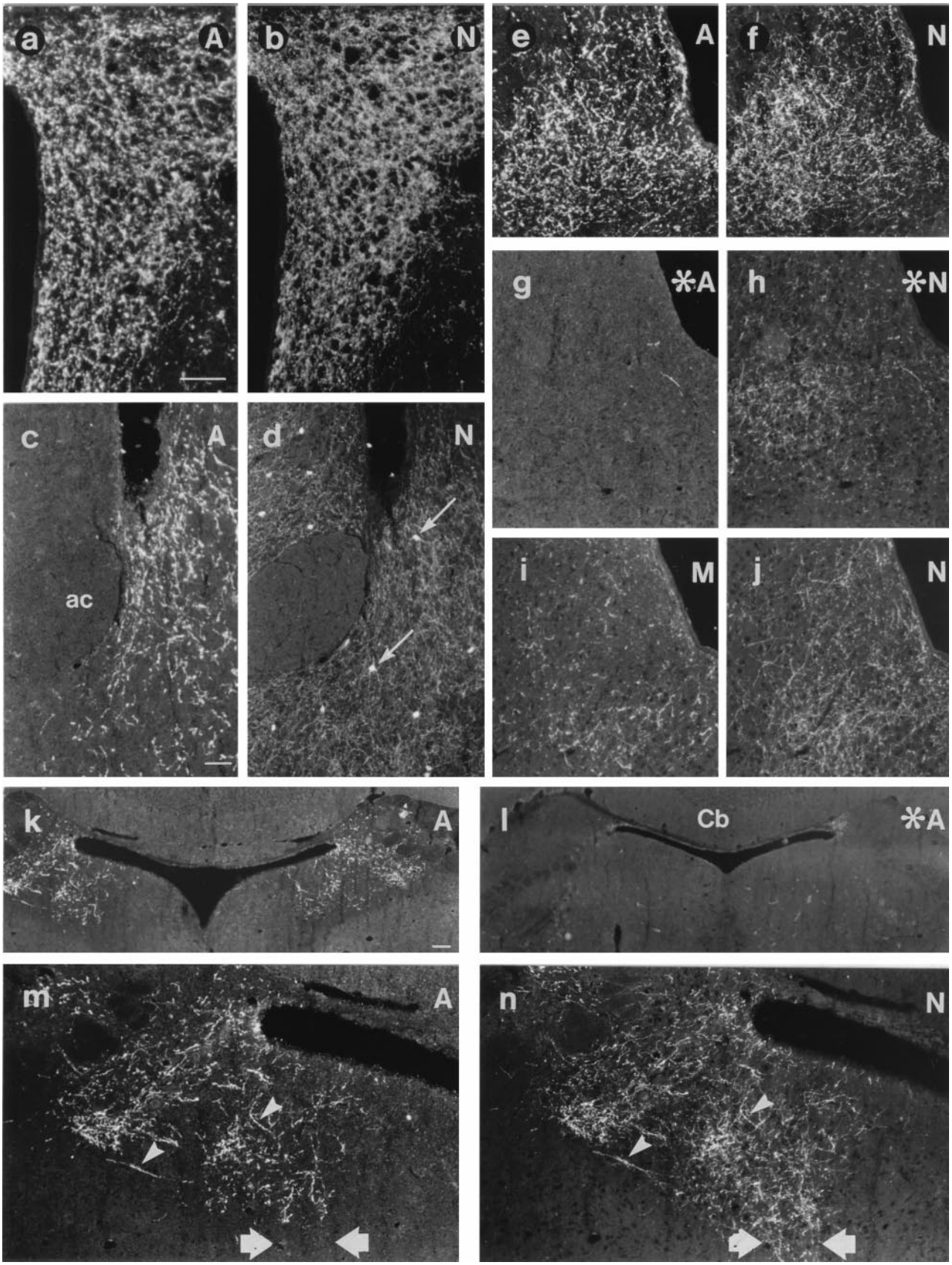

FIG. 2. Micrographs from sections of mouse brain processed for double-labeling immunohistochemistry for AGRP (A; *a*, *c*, *e*, *g*, *k*, *l*, and *m*), NPY (N; *b*, *d*, *f*, *h*, *j*, and *n*), or αMSH (M; *i*) showing the PVH (*a* and *b*), bed nucleus of the stria terminalis (BST; *c* and *d*), periaqueductal gray (*e*–*j*), and PBN (*k*–*n*) from normal (*a*–*f*, *i*–*k*, *m*, and *n*) or MSG-treated (asterisk; *g*, *h*, and *l*) mice. Note colocalization of AGRP and NPY in several fibers (arrowheads in *m* and *n*), but not in cell bodies of the BST (thin arrows in *d*), or in NPY fibers of the central gray of the pons (thick arrows in *m* and *n*). MSG treatment virtually abolishes AGRP (*g*) and decreases NPY staining (*h*). ac, anterior commissure; Cb, cerebellum. [Bar in $a = 50\ \mu$m (*a*, *b*, *e*–*j*, *m*, and *n*); in $c = 50\ \mu$m (*c* and *d*); and in $k = 100\ \mu$m (*k* and *l*).]

approximately half of the NPY-ir terminals stained for AGRP. The medial preoptic area, including the vascular organ of the lamina terminalis and anteroventral periventricular nucleus, contained a high-density network with moderate to low densities in the lateral preoptic area. High-density networks were observed in the periventricular area and covering the A13 dopamine cell group. Both parvo- and magnocellular regions of the paraventricular nucleus (PVH) contained a high density of fibers (Fig. 2*a*), with a low-density network in the supraoptic nucleus. The entire arcuate nucleus (Figs. 1*f* and 3 *a* and *c*), the perifornical area, and the dorsomedial nucleus (excluding the pars compacta) contained high-density networks (Fig. 3*a*). Moderate to low fiber density was observed in the lateral hypothalamic area including the magnocellular nucleus. Fiber density was low to moderate in the posterior hypothalamic area and moderate in the medial tuberal nucleus. AGRP-LI was absent from the suprachiasmatic, ventromedial, and mammillary nuclei, as well as the median eminence (Fig. 3*a*). In the thalamus, AGRP-ir terminals were observed only in the xiphoid (low density) and paraventricular (high density) nuclei. Fiber density in the zona incerta was low.

In the mesencephalon, the paranigral nucleus and ventral tegmental area contained moderately dense fiber networks, with scattered fibers in the substantia nigra, pars compacta. Terminal networks were observed in the rostral and central linear, ventral and inferior dorsal raphe nuclei (high to moderate density), and the retrorubral field (A8; moderate density). High fiber density was seen in the rostral (Bregma −4.0) part of the lateral periaqueductal gray (Fig. 2*e*) and in the dorsomedial tegmental area, with single fibers throughout the remaining periaqueductal gray. Fibers formed a high-density network in the laterodorsal tegmental nucleus continuing into the lateral parabrachial nucleus (PBN). However, the NPY-ir fibers in the neighboring Kölliker–Fuse nucleus did not stain for AGRP.

In the pons, high-density terminal networks were observed in the medial and, in particular, in more rostral sections (Bregma −5.3), lateral PBN, where almost all NPY-ir terminals stained for AGRP, extending into Barrington's nucleus (Fig. 2*k* and cf. Fig. 2 *m* with *n*). However, the intensely NPY-ir network in the ventral central gray of the pons appeared to stain for AGRP (cf. Fig. 2 *m* with *n*). Occasional fibers were observed just ventral to the fourth ventricle and coursing through the superior cerebellar peduncle.

In the medulla oblongata and spinal cord, only occasional fibers in the dense NPY-ir network of the dorsal lateral and medial regions of the nucleus of the solitary tract (NTS) stained for AGRP.

Double-staining for NPY and αMSH showed immunoreactivity for these two markers in separate fiber populations, but these terminals were intermingled in all areas in which AGRP-LI was observed (cf. Fig. 2 *i* with *j*).

MSG-treated mice displayed increased adiposity, stunted growth, and atrophic pituitaries and optic nerves. Cresyl violet-counterstained sections from the hypothalamus of MSG-treated mice revealed a marked shrinkage of the arcuate nucleus, widening of the third ventricle, and a thinning of the median eminence. Histochemically, a virtually complete disappearance of AGRP-ir arcuate cell bodies and terminals was observed (cf. Fig. 2 *e* and *k* with *g* and *l*, respectively). However,

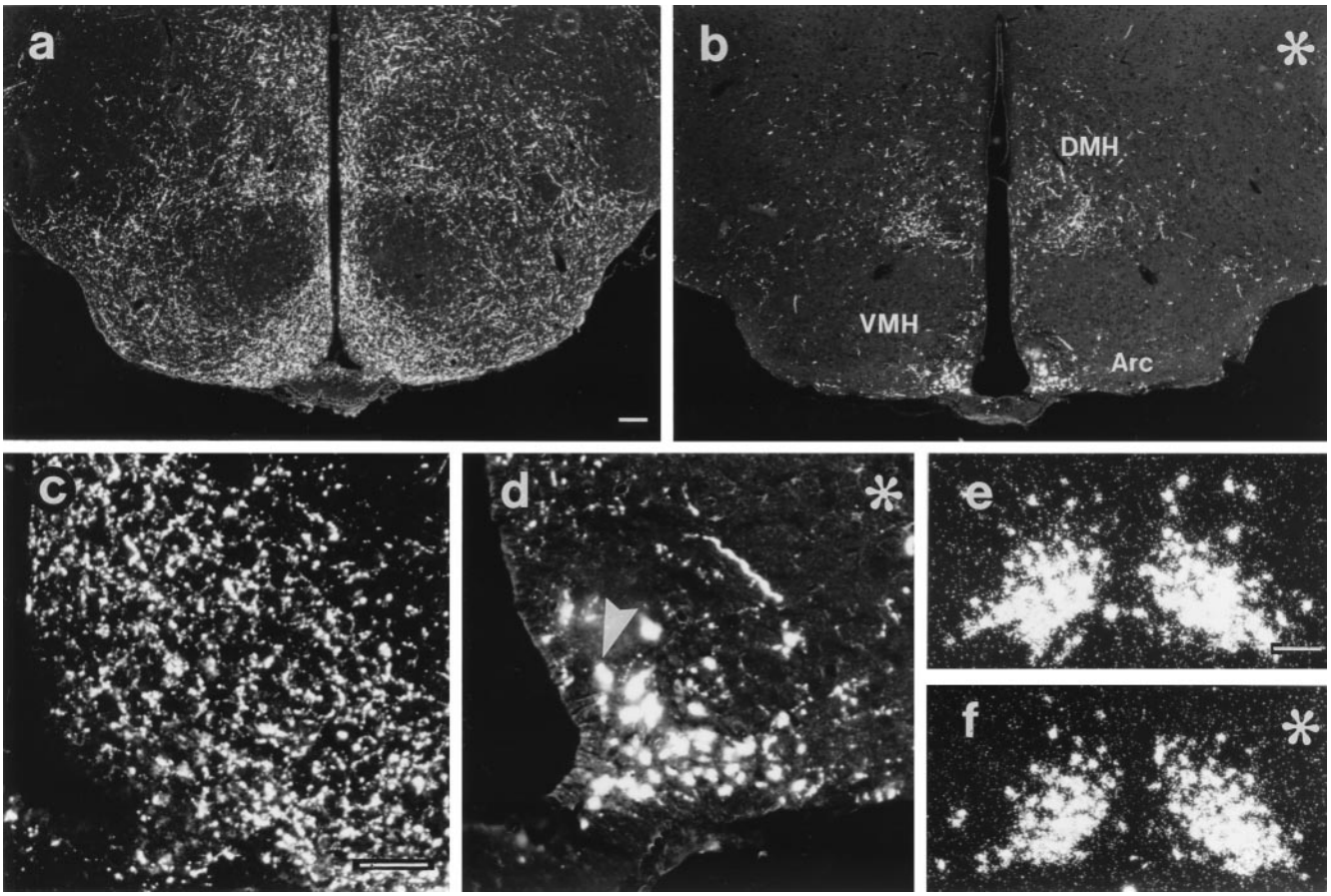

FIG. 3. Fluorescence (*a*– *d*) and dark-field (*e* and *f*) micrographs from arcuate nucleus sections processed for immunohistochemistry (*a*– *d*) or *in situ* hybridization (*e* and *f*) showing AGRP peptide (*a*– *d*) or mRNA (*e* and *f*), respectively, from *anx*/*anx* (asterisk; *b*, *d*, and *f*) and control (*a*, *c*, and *e*) mice. AGRP staining in *anx*/*anx* mice is decreased in hypothalamic terminals (cf. *a* with *b*), increased in arcuate cell bodies (arrowhead; cf. *c* with *d*), whereas AGRP mRNA is unchanged (cf. *e* with *f*). Arc, arcuate; DMH, dorsomedial nucleus; VMH, ventromedial nucleus. [Bar in *a* = 100 μm (*a* and *b*), in *c* = 50 μm (*c* and *d*), and in *e* = 50 μm (*e* and *f*).]

immunohistochemical staining for NPY in brains from these animals showed that many areas, e.g., the PVH, showed essentially normal NPY staining, although no NPY-ir cell bodies could be found in the arcuate and NPY-ir terminals were decreased in number in several areas, including the preoptic, arcuate, periaqueductal (cf. Fig. 2 *f* with *h*), and parabrachial nuclei.

In *anx/anx* mice, strongly AGRP-ir cell bodies, not seen in littermate controls, were observed in the arcuate nucleus (cf. Fig. 3 *a* and *c* with *b* and *d*, respectively). The number of AGRP-ir fibers in the dorsal part of the dorsomedial hypothalamic nucleus was decreased significantly by 41.6 ± 5.0% in *anx/anx* mice (Fig. 4; cf. Fig. 3 *a* with *b*). Similar and even larger decreases in AGRP-ir terminals were observed in other areas examined, e.g., the preoptic area, arcuate nucleus (cf. Fig. 3 *c* with *d*), periaqueductal gray, and the PBN. In contrast, AGRP mRNA levels in the arcuate, as quantified from film autoradiographs, were not significantly different in *anx/anx* as compared with control littermates (105.5 ± 0.1% of control; $n = 5$; cf. Fig. 3 *e* and *f*).

DISCUSSION

The many NPY-expressing cell populations in the brain (2, 3) give rise to extensive, multiple, and overlapping terminal networks. Thus, it has been difficult to assess which of these terminals originate from the arcuate nucleus. Here we use an indirect approach to delineate the brain regions targeted by arcuate NPY neurons, using AGRP as a marker. Shutter *et al.* (15) first demonstrated the similar expression patterns of AGRP and NPY in adjacent sections of the arcuate nucleus. Recently, using double-labeling methodology, a high degree of coexpression of AGRP and NPY has been demonstrated in arcuate cells in the mouse by *in situ* hybridization (13) and in the rat by immunohistochemistry (14). The present report on mouse confirms and extends these studies by demonstrating the presence of AGRP-LI in NPY-ir arcuate cell bodies and widespread terminals. In fact, the present results show that no other AGRP mRNA-expressing cells were found in the brain, supporting a previous *in situ* hybridization report (15), nor were any other AGRP-ir cell bodies seen after colchicine treatment, nor were AGRP-positive, NPY-negative terminals observed. Finally, in two models affecting the arcuate nucleus leading to a decrease in NPY-ir terminals, the MSG-treated (11, 19) and *anx/anx* (9) mice, respectively, a marked and sometimes almost complete disappearance of AGRP-ir terminals could be seen in all brain regions. Taken together, the present data suggest that the presence of AGRP-LI may be a selective marker for arcuate nucleus-derived NPY terminals and show that the small-sized arcuate NPY/AGRP neurons have much wider projections than perhaps previously assumed. In fact, they largely follow the large-sized melanocortin neurons in the arcuate (see below) and partly parallel the orexin/hypocretin and melanin-concentrating hormone neurons in the lateral–dorsal hypothalamus (28). We also noted that despite the elimination of AGRP-LI, many areas still exhibited substantial NPY-ir terminal networks after MSG treatment, supporting the view that many brain nuclei receive NPY inputs from several sources as shown by Bai *et al.* (10) and Sawchenko *et al.* (29). There is evidence that extraarcuate sources may increase their innervation as the arcuate contribution decreases. Thus, ectopic expression of NPY in the PVH has been demonstrated in MSG-treated rats (19).

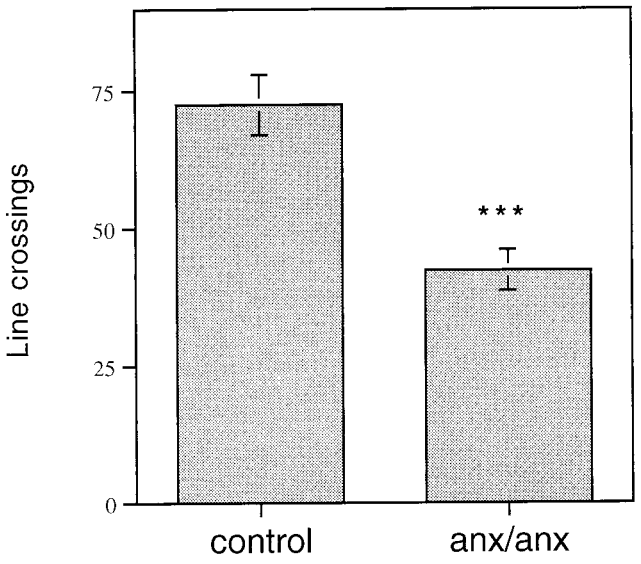

FIG. 4. Quantification of line crossings (see *Materials and Methods*) of AGRP fibers in the dorsomedial hypothalamic nucleus of *anx/anx* mice ($n = 10$) and control littermates ($n = 7$). The density of AGRP terminals is decreased significantly in *anx/anx* mice. ***, $P < 0.001$.

The dramatically altered AGRP histochemistry in anorectic *anx/anx* mice, with decreased AGRP-LI in terminals and a pronounced increase in cell bodies but normal AGRP mRNA levels, parallels the NPY histochemistry in these animals (9). These findings strongly suggest that the phenotype of this mutant may be related to the arcuate neurons themselves, rather than to a particular neuropeptide gene/peptide.

Previous reports on the distribution of melanocortinergic projections have described a large number of targeted brain areas (30) that are similar to the anatomical localization of AGRP-ir fibers as described in the present report. However, notable exceptions exist, e.g., the NTS that receives a dense melanocortinergic projection but only occasional AGRP-ir fibers. We observed an intermingling of AGRP- and αMSH-ir terminals in many nuclei, providing morphological evidence that melanocortin release may be balanced with release of their endogenous antagonist AGRP in these areas. It has been demonstrated that melanocortin neurons express the NPY Y1 receptor (24, 31) and that these cells receive innervation from NPY terminals (24, 32). Thus, arcuate NPY cells could inhibit melanocortin activity (*i*) at the cell body level through the Y1 receptor and (*ii*) postsynaptically by release of AGRP, supporting previously described antagonistic actions of NPY and melanocortins on food intake (17).

The arcuate nucleus possesses receptors for insulin (33), leptin (34, 35), growth hormone (36), glucocorticoids (37), and sex hormones (38) and thus may serve as a relay station for long-term information relating to the metabolic state of the individual. In contrast, the NTS is the termination area of the vagus nerve and receives viscerosensory information, e.g., gastric and gustatory primary sensory inputs (39), that serves as a short-term regulator of food intake (40). The NTS projects to the PBN (41), periaqueductal gray (42), central nucleus of the amygdala, bed nucleus of the stria terminalis, median preoptic, paraventricular and dorsomedial hypothalamic nuclei, as well as the lateral hypothalamic area (43, 44). While the paucity of AGRP terminals in the NTS would dispute a major influence at the cell body level of NTS neurons, we noted a striking convergence of the projections of AGRP/NPY cells and those described for the NTS, suggesting that integration of short- and long-term satiety signals may occur at multiple downstream sites.

One area innervated by both the NTS and the arcuate is the PBN, which receives inputs from four major sources: brain stem (41), basal forebrain, hypothalamus, and cerebral cortex (45), implicating it as a major integrator of peripheral signals. In turn, the PBN relays information to the thalamus and cortex (46). In addition to the gastric and gustatory afferents (47), a role for this circuitry in food-intake regulation is supported by lesion experiments (48). The present results suggest that

arcuate NPY may regulate PBN activity. An arcuate-PBN projection has been described previously (45, 49, 50), but the contribution of NPY therein was not investigated.

The present data suggest that arcuate NPY neurons project to a large number of sites both within and outside of the hypothalamus. The presence of AGRP in these projections and their noteworthy resemblance to arcuate-derived melanocortinergic pathways, as well as their convergence with NTS-derived pathways, indicate postsynaptic interactions of signals from these populations.

This study was supported by the Swedish Medical Research Council (04X-2887, 3X-10909), Marianne and Marcus Wallenberg's Foundation, Knut and Alice Wallenbergs Stiftelse, Astra Arcus AB, an unrestricted Neuroscience Grant from Bristol-Myers Squibb, NARSAD, and funds from Karolinska Institutet and the Karolinska Hospital. We are grateful to Dr. Claude Bohuon, Institut Gustave Roussy, Villejuif, France, for NPY mAbs. We thank Dr. Richard Thompson for valuable comments.

1. Tatemoto, K., Carlquist, M. & Mutt, V. (1982) *Nature (London)* **296,** 659–660.
2. Chronwall, B. M., DiMaggio, D. A., Massari, V. J., Pickel, V. M., Ruggiero, D. A. & O'Donohue, T. L. (1985) *Neuroscience* **15,** 1159–1181.
3. de Quidt, M. E. & Emson, P. C. (1986) *Neuroscience* **18,** 545–618.
4. Clark, J. T., Kalra, P. S., Crowley, W. R. & Kalra, S. P. (1984) *Endocrinology* **115,** 427–429.
5. Stanley, B. G. & Leibowitz, S. F. (1985) *Proc. Natl. Acad. Sci. USA* **82,** 3940–3943.
6. Sahu, A., Kalra, P. S. & Kalra, S. P. (1988) *Peptides* **9,** 83–86.
7. Brady, L. S., Smith, M. A., Gold, P. W. & Herkenham, M. (1990) *Neuroendocrinology* **52,** 441–447.
8. Frankish, H. M., Dryden, S., Hopkins, D., Qang, Q. & Williams, G. (1995) *Peptides* **4,** 757–771.
9. Broberger, C., Johansen, J., Schalling, M. & Hökfelt, T. (1997) *J. Comp. Neurol.* **387,** 124–135.
10. Bai, F. L., Yamano, M., Shiotani, Y., Emson, P. C., Smith, A. D., Powell, J. F. & Tohyama, M. (1985) *Brain Res.* **331,** 172–175.
11. Meister, B., Ceccatelli, S., Hökfelt, T., Andén, N.-E. & Theodorsson, E. (1989) *Exp. Brain Res.* **76,** 343–368.
12. Baker, R. A. & Herkenham, M. (1995) *J. Comp. Neurol.* **358,** 518–530.
13. Hahn, T. M., Breininger, J. F., Baskin, D. G. & Schwartz, M. W. (1998) *Nat. Neurosci.* **1,** 271–272.
14. Broberger, C., De Lecea, L., Sutcliffe, J. G. & Hökfelt, T. (1998) *J. Comp. Neurol.* **402,** 460–474.
15. Shutter, J. R., Graham, M., Kinsey, A. C., Scully, S., Lüthy, R. & Stark, K. L. (1997) *Genes Dev.* **11,** 593–602.
16. Ollmann, M. M., Wilson, B. D., Yang, Y.-K., Kerns, J. A., Chen, Y., Gantz, I. & Barsh, G. S. (1997) *Science* **278,** 135–138.
17. Fan, W., Boston, B. A., Kesterson, R. A., Hruby, V. J. & Cone, R. D. (1997) *Nature (London)* **385,** 165–168.
18. Olney, J. W. (1969) *Science* **164,** 719–721.
19. Kerkérian, L. & Pelletier, G. (1986) *Brain Res.* **369,** 388–390.
20. Potts, A. M., Modrell, R. W. & Kingsbury, C. (1960) *Am. J. Ophtalmol.* **50,** 900–907.
21. Larhammar, D., Ericsson, A. & Persson, H. (1987) *Proc. Natl. Acad. Sci. USA* **84,** 2068–2072.
22. Schmitz, G. G., Walter, T., Seibl, R. & Kessler, C. (1991) *Anal. Biochem.* **192,** 222–231.
23. Broberger, C., Landry, M., Wong, H., Walsh, J. & Hökfelt, T. (1997) *Neuroendocrinology* **66,** 393–408.
24. Dagerlind, Å., Friberg, K., Bean, A. & Hökfelt, T. (1992) *Histochemistry* **98,** 39–49.
25. Schalling, M., Seroogy, K., Hökfelt, T., Chai, S.-Y., Hallman, H., Persson, H., Larhammar, D., Ericsson, A., Terenius, L., Graffi, J., Massoulié, J. & Goldstein, M. (1988) *Neuroscience* **24,** 337–349.
26. Grouzmann, E., Comoy, E., Walker, P., Burnier, M., Bohuon, C., Waeber, B. & Brunner, H. (1992) *Hybridoma* **11,** 409–424.
27. Franklin, K. B. J. & Paxinos, G. (1997) *The Mouse Brain in Stereotaxic Coordinates* (Academic, San Diego).
28. Sawchenko, P. E. (1998) *J. Comp. Neurol.*, in press.
29. Sawchenko, P. E., Swanson, L. W., Grzanna, R., Howe, P. R. C., Bloom, S. R. & Polak, J. M. (1985) *J. Comp. Neurol.* **241,** 138–153.
30. Khachaturian, H. Y., Lewis, M. E., Tsou, K. & Watson, S. J. (1985) in *Handbook of Chemical Neuroanatomy*, eds. Björklund, A. & Hökfelt, T. (Elsevier, Amsterdam), Vol. 4, pp. 216–272.
31. Fuxe, K., Tinner, B., Caberlotto, L., Bunnemann, B. & Agnati, L. F. (1997) *Neurosci. Lett.* **225,** 49–52.
32. Csiffáry, A., Görcs, T. J. & Palkovits, M. (1990) *Brain Res.* **506,** 215–222.
33. Marks, J. L., Porte, J. D., Stahl, W. L. & Baskin, D. G. (1990) *Endocrinology* **127,** 3234–3236.
34. Mercer, J. G., Hoggard, N., Williams, L. M., Lawrence, C. B., Hannah, L. T., Morgan, P. J. & Trayhurn, P. (1996) *J. Neuroendocrinol.* **8,** 733–735.
35. Håkansson, M.-L., Brown, H., Ghilardi, N., Skoda, R. C. & Meister, B. (1998) *J. Neurosci.* **18,** 559–572.
36. Kamegai, J., Minami, S., Sugihara, H., Hasegawa, O., Higuchi, H. & Wakabayashi, I. (1996) *Endocrinology* **137,** 2109–2112.
37. Hisano, S., Kagotani, Y., Tsuruo, Y., Daikoku, S., Chihara, K. & Whitnall, M. H. (1988) *Neurosci. Lett.* **95,** 13–18.
38. Sar, M., Sahu, A., Crowley, W. R. & Kalra, S. P. (1990) *Endocrinology* **127,** 2752–2756.
39. Cechetto, D. F. (1987) *FASEB J.* **46,** 17–23.
40. Woods, S. C., Seeley, R. J., Porte, D., Jr., & Schwartz, M. W. (1998) *Science* **280,** 1378–1383.
41. Herbert, H., Moga, M. M. & Saper, C. B. (1990) *J. Comp. Neurol.* **293,** 540–580.
42. Herbert, H. & Saper, C. B. (1992) *J. Comp. Neurol.* **315,** 34–52.
43. Ricardo, J. A. & Koh, E. T. (1978) *Brain Res.* **153,** 1–26.
44. ter Horst, G. J., de Boer, P., Luiten, P. G. M. & van Willigen, J. D. (1989) *Neuroscience* **31,** 785–797.
45. Moga, M. M., Herbert, H., Hurley, K. M., Yasui, Y., Gray, T. S. & Saper, C. B. (1990) *J. Comp. Neurol.* **295,** 624–661.
46. Cechetto, D. F. & Saper, C. B. (1987) *J. Comp. Neurol.* **262,** 27–45.
47. Hermann, G. E. & Rogers, R. C. (1985) *J. Auton. Nerv. Syst.* **13,** 1–17.
48. Edwards, G. L. & Ritter, R. C. (1989) *Am. J. Physiol.* **256,** R306–R312.
49. Moga, M. M., Saper, C. B. & Gray, T. S. (1990) *J. Comp. Neurol.* **295,** 662–682.
50. Sim, L. J. & Joseph, S. A. (1991) *J. Chem. Neuroanat.* **4,** 97–109.